Skin microdialysis detects distinct immunologic patterns in chronic inflammatory skin diseases

Moritz Maximilian Hollstein, MD, Stephan Traidl, MD, Anne Heetfeld, MD, Susann Forkel, MD, Andreas Leha, PhD, Natalia Alkon, PhD, et al

GRAPHICAL ABSTRACT

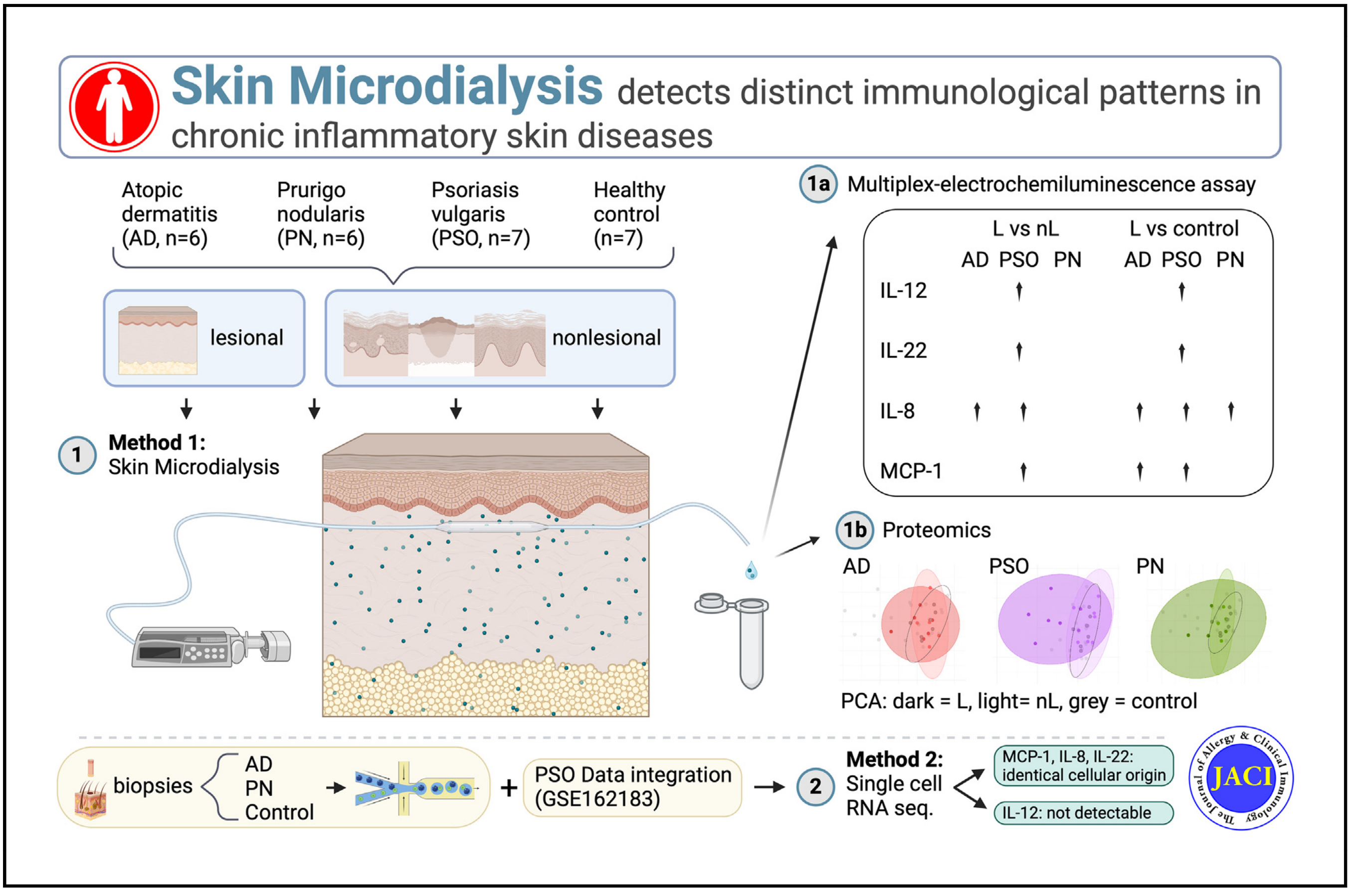

Capsule summary: Skin microdialysis is a valuable tool to analyze inflammatory skin lesions, revealing that in atopic dermatitis, unlike psoriasis vulgaris and prurigo nodularis, nonlesional skin exhibits characteristics of lesional skin.

J Allergy Clin Immunol 2024;154:1450-61.

https://doi.org/10.1016/j.jaci.2024.06.024

Skin microdialysis detects distinct immunologic patterns in chronic inflammatory skin diseases

Moritz Maximilian Hollstein, MD,[a] Stephan Traidl, MD,[b] Anne Heetfeld, MD,[a] Susann Forkel, MD,[a] Andreas Leha, PhD,[c] Natalia Alkon, PhD,[d] Jannik Ruwisch, MD,[e] Christof Lenz, PhD,[f,g] Michael Peter Schön, MD,[a] Martin Schmelz, MD,[h] Patrick Brunner, MD, MSc,[i] Martin Steinhoff, MD, PhD,[j] and Timo Buhl, MD[a] *Göttingen, Hannover, and Mannheim, Germany; Vienna, Austria; New York, NY; and Doha, Qatar*

Background: Insight into the pathophysiology of inflammatory skin diseases, especially at the proteomic level, is severely hampered by the lack of adequate *in situ* data.

Objective: We characterized lesional and nonlesional skin of inflammatory skin diseases using skin microdialysis.

Methods: Skin microdialysis samples from patients with atopic dermatitis (AD, n = 6), psoriasis vulgaris (PSO, n = 7), or prurigo nodularis (PN, n = 6), as well as healthy controls (n = 7), were subjected to proteomic and multiplex cytokine analysis. Single-cell RNA sequencing of skin biopsy specimens was used to identify the cellular origin of cytokines.

Results: Among the top 20 enriched Gene Ontology (GO; geneontology.org) annotations, nicotinamide adenine dinucleotide metabolic process, regulation of secretion by cell, and pyruvate metabolic process were elevated in microdialysates from lesional AD skin compared with both nonlesional skin and controls. The top 20 enriched Kyoto Encyclopedia of Genes and Genomes (KEGG; genome.jp/kegg) pathways in these 3 groups overlapped almost completely. In contrast, nonlesional skin from patients with PSO or PN and control skin showed no overlap with lesional skin in this KEGG pathway analysis. Lesional skin from patients with PSO, but not AD or PN, showed significantly elevated protein levels of MCP-1 compared with nonlesional skin. IL-8 was elevated in lesional versus nonlesional AD and PSO skin, whereas IL-12p40 and IL-22 were higher only in lesional PSO skin. Integrated single-cell RNA sequencing data revealed identical cellular sources of these cytokines in AD, PSO, and PN.

Conclusion: On the basis of microdialysates, the proteomic data of lesional PSO and PN skin, but not lesional AD skin, differed significantly from those of nonlesional skin. IL-8, IL-22, MCP-1, and IL-12p40 might be suitable markers for minimally invasive molecular profiling. (J Allergy Clin Immunol 2024;154:1450-61.)

***Key words:** Microdialysis, pruritus, atopic dermatitis, psoriasis vulgaris*

Autoimmune and inflammatory skin disorders are noninfectious diseases with a complex immune-mediated pathophysiology.[1] One method to classify these diseases is based on cytokine profiles and T helper cell involvement. Type 1 immune responses may induce keratinocyte necroptosis in an IFN-γ–dependent manner in certain autoimmune diseases, such as lupus erythematosus or lichen planus.[1] The physiologic role of this type of immune responses may involve defense against intracellular bacteria and protozoa, as well as viruses.[2] Type 2 immune responses induce IgE-producing plasma cells and pruritus, the latter via cytokines such as IL-31.[3,4] They are important for venom neutralization, protection against parasites, tissue repair, and tissue fibrosis; these responses play critical roles in allergic diseases such as atopic dermatitis (AD).[2,5,6] Type 3 immune responses are mediated primarily by IL-22, IL-17A, and IL-17F.[2] These cytokines mediate epidermal proliferation (acanthosis) as well as recruitment of neutrophils and antimicrobial peptide synthesis.[2] These mechanisms aid in defense against extracellular bacteria and fungi. Type 3 immune responses are also involved in the pathogenesis of psoriasis vulgaris (PSO).[7] Assessing lesional cytokine profiles is difficult through conventional diagnostics such as histopathologic classification of lesional skin including immune cell infiltrates. Thus, although cytokine profiles are used in basic research, they do not aid routine diagnostics.

Furthermore, for some diseases, such as AD, several endotypes have been proposed that cannot be distinguished by conventional diagnostic methods.[8] In PSO and AD, overlapping phenotypes have been described, resulting in misdiagnosis; these phenotypes are sometimes referred to as psoriasiform eczema, eczematous PSO, or sebopsoriasis.[9,10] Furthermore, in AD, nonlesional skin shares many characteristics with lesional skin, such as barrier defects and T-cell infiltrates, and it can be as pruritic as lesional skin.[11-13] Thus, an improved, minimally invasive toolbox would be highly desirable to detect inflammatory patterns for more accurate diagnosis.

From [a]the Department of Dermatology, Venereology and Allergology, University Medical Centre Göttingen (UMG), Göttingen; [b]the Department of Dermatology and Allergy, Hannover Medical School, Hannover; [c]the Department of Medical Statistics, UMG, Göttingen; [d]the Department of Dermatology, Medical University of Vienna, Vienna; [e]the Clinic for Respiratory Medicine, Hannover Medical School, Hannover; [f]the Department of Clinical Chemistry, UMG, Göttingen; [g]the Bioanalytical Mass Spectrometry, Max Planck Institute for Multidisciplinary Sciences, Göttingen; [h]the Department of Experimental Pain Research, MCTN, Medical Faculty Mannheim, University of Heidelberg, Mannheim; [i]the Department of Dermatology, Icahn School of Medicine at Mount Sinai, New York; and [j]the Department of Dermatology and Venereology, Hamad Medical Corporation, Doha.

Received for publication December 4, 2023; revised April 24, 2024; accepted for publication June 4, 2024.

Available online August 12, 2024.

Corresponding author: Moritz Hollstein, MD, University Medical Center Göttingen, Department of Dermatology, Venereology and Allergology, Robert Koch Str 40, 37075 Göttingen, Germany. E-mail: moritz.hollstein@med.uni-goettingen.de.

0091-6749

https://doi.org/10.1016/j.jaci.2024.06.024

Abbreviations used
AD: Atopic dermatitis
CCL: Chemokine C-C motif ligand
CXCL: C-X-C motif chemokine ligand
EASI: Eczema Area and Severity Index
FWHM: Full width at half maximum
GO: Gene Ontology (geneontology.org)
KEGG: Kyoto Encyclopedia of Genes and Genomes (genome.jp/kegg)
LC-MS/MS: Liquid chromatography–MS/MS
MCP: Monocyte chemotactic protein
MIP: Macrophage inflammatory protein
MS: Mass spectrometry
MS/MS: Tandem MS
PASI: Psoriasis Area and Severity Index
PCA: Principal component analysis
PN: Prurigo nodularis
PSO: Psoriasis vulgaris
scRNA-Seq: Single-cell RNA sequencing
SWATH: Sequential windowed acquisition of all theoretical fragment ions
TSLP: Thymic stromal lymphopoietin

Current options to characterize inflammatory skin diseases are based on molecular disease classifiers at the genetic level or through omics.[14,15] These procedures generally require skin biopsies to be performed and are time-consuming and costly. We hypothesized that classification and diagnosis of inflammatory skin diseases might be performed on the basis of protein expression rather than genetic or transcriptomic analyses. We further hypothesized that quantifying individual proteins (including cytokines and chemokines) as well as other soluble components in the intercellular space might enable disease profiling, thus allowing invasive skin biopsies to be avoided in the future.

To collect samples for minimally invasive extracellular protein analysis, we performed skin microdialysis. The procedure involves penetrating the patient's dermis with a semipermeable polycarbonate membrane and subsequent perfusion. Relevant soluble components penetrate through pores into the dialysate.[16-18] Microdialysis causes little pain, leaves no scar, and can be repeated in the same location, in contrast to punch biopsies of the skin. We demonstrate the feasibility of skin microdialysis as a minimally invasive diagnostic tool for profiling the inflammatory skin diseases AD, PSO, and prurigo nodularis (PN). Furthermore, by comparing lesional with nonlesional skin of patients and with skin of healthy controls, we propose disease markers (cytokines and chemokines) locally at the protein level.

METHODS

After obtaining informed consent, we performed skin microdialysis on 26 volunteers with AD (n = 6), PSO (n = 7), or PN (n = 6), and healthy controls (n = 7). Additional patient samples of 3 patients with prurigo simplex subacuta were used for generating the proteomic library. The Eczema Area and Severity Index (EASI) score was determined for all patients with AD, and the Psoriasis Area and Severity Index (PASI) score was determined for all patients with PSO before the microdialysis procedure. In all patients, Dermatology Life Quality Index (DLQI) was evaluated, and pruritus was assessed on an 11-point visual analog scale. This study was conducted in accordance with the World Medical Association's Declaration of Helsinki; it was reviewed and approved by the local ethics committee (approval 31/11/17). Data sets are available online (www.ebi.ac.uk/pride/archive/projects/PXD050245).

Skin microdialysis

The microdialysis procedure was performed as previously described.[16] Catheter tubes were custom made in the laboratory of Martin Schmelz. Catheters were hollow fibers (0.4 mm in diameter with a pore-size cutoff of 3000 kDa). Patients were seated in a comfortable position in a temperature- and humidity-controlled environment for at least 20 minutes before the start of the procedure (see Fig E1, *A,* in this article's Online Repository available at www.jacionline.org). A 25-gauge cannula connected to the hollow fiber and an attached flexible tube were prepared in a germ-reduced environment (Fig E1, *B*). The cannula was inserted intradermally over a distance of 1 cm at the area of interest located on an extremity, primarily the upper arm. We sampled lesional skin; nonlesional skin—that is, skin without visible lesions; and skin of healthy controls (Fig E1, *C* and *D*). The attached hollow fiber was threaded through the skin. This procedure was generally well tolerated, and no local anesthesia was required. The correct intracutaneous positioning of the catheter was verified, and the needle was detached from the catheter by cutting the catheter at the outflow side (see Fig E2, *A,* in the Online Repository). Ringer solution (B. Braun, Melsungen, Germany) was perfused at a rate of 5 μL/min with a syringe pump (CMA 4004; Harvard Apparatus, Holliston, Mass) via a Tygon tube (Novodirekt, Kehl, Germany). A microcentrifuge tube (1.5 mL) was positioned just below the loose end of the catheter to collect the dialysate (Fig E2, *B*). In the 40-minute sampling period, 2 dialysate samples were collected, one every 20 minutes.

Proteomics mass spectrometry sample preparation

For proteomic analysis, samples from 6 patients with AD, 7 patients with PSO, 4 patients with PN, and 7 healthy controls were available. Two samples from patients with PN could not be included because of technical issues. For each disease, lesional and nonlesional dialysates were evaluated in technical duplicates. Proteins were extracted, purified, and digested with tryptase according to a magnetic bead-based SP3 protocol.[19] Digested peptides were dried in a SpeedVac instrument and stored at −20°C until further analysis. For generation of a peptide library, equal aliquots from each sample were pooled to a total amount of 200 μg and separated into 12 fractions with basic pH reverse-phase C_{18} separation on a fast protein liquid chromatography system (äkta pure; Cytiva Lifesciences, Marlborough, Mass) with a 36/3 staggered pooling scheme. All samples were spiked with a synthetic peptide standard used for retention time alignment (iRT Standard, Schlieren, Switzerland).

Protein digests were analyzed on a nanoflow chromatography system (Eksigent nanoLC425) connected to a hybrid triple quadrupole-TOF mass spectrometer (TripleTOF 5600+) equipped with a NanoSpray III ion source (ion spray voltage 2400 V; interface heater temperature 150°C; sheath gas setting 12) and controlled by Analyst TF 1.7.1 software, build 1163 (all AB Sciex, Framingham, Mass). In brief, peptides were dissolved in loading buffer (2% acetonitrile and 0.1% formic acid in water) to a concentration of 0.3 μg/μL. For each analysis, 1.5 μg protein was enriched on a self-packed precolumn (0.15 mm ID × 20 mm, Reprosil-Pur120 C_{18}-AQ 5 μm, Dr Maisch, Ammerbuch-Entringen, Germany) and separated on an analytical RP-C_{18} column (0.075 mm ID × 200 mm, Reprosil-Pur 120 C_{18}-AQ, 3 μm, Dr Maisch) with a 100-minute linear gradient of 5-35% acetonitrile/0.1% formic acid (vol/vol) at 300 nL/min.

Samples were normalized to same protein amounts loaded onto the liquid chromatography–tandem mass spectrometry (LC-MS/MS) system before analysis and using a total area sums approach following protein quantitation. Qualitative LC-MS/MS analysis was performed with a top 30 data-dependent acquisition method with an MS survey scan of *m/z* 380-1250 over 250 ms, at a resolution of 35,000 full width at half maximum (FWHM). MS/MS scans of *m/z* 180-1500 were accumulated over 100 ms at a resolution of 17,500 FWHM and a precursor isolation width of 0.7 FWHM, thus resulting in a total cycle time of 3.4 seconds. Precursors above a threshold mass spectrometry intensity of 200 cps with charge states of 2^+, 3^+, and 4^+ were selected for MS/MS. The dynamic exclusion time was set to 15 s. MS/MS activation was achieved by collision-induced dissociation, using nitrogen as a collision gas and the manufacturer's default rolling collision energy settings. Two biological replicates per sample were analyzed to construct a spectral library.

For quantitative SWATH (sequential windowed acquisition of all theoretical fragment ions) analysis, MS/MS data were acquired with 100 variable size windows[20] across the range *m/z* 400-1200. Fragments were produced with rolling collision energy settings for charge state 2^+, and fragments were acquired across the range *m/z* 180-1500 for 40 ms per segment. Inclusion of a 250 ms survey scan resulted in an overall cycle time of 4.3 seconds. Two replicate injections were acquired for each of the 2 biological replicates of the 4 samples.

Protein identification was performed in ProteinPilot v5.0, build 4304, software (AB Sciex) with "thorough" settings. All MS/MS spectra from qualitative analyses were searched against the UniProtKB *Homo sapiens* reference proteome (revision 01-2020) augmented with a set of 51 known common laboratory contaminants.

SWATH peak extraction was achieved in PeakView v2.1, build 11041 (AB Sciex), with the SWATH quantification microApp v2.0, build 2003. After retention time correction on endogenous peptides spanning the entire retention time range, peak areas were extracted with information from the MS/MS library.[21] The resulting peak areas were then summed to peptide and finally protein area values, which were used for further statistical analysis.

Multiplex electrochemiluminescence assay

Frozen, undiluted samples were thawed and measured with a customized U-Plex assay (Meso Scale Discovery, Rockville, Md) featuring 3 multiplex plates. Plate 1 contained TNF-α, IFN-γ, IL-1β, IL-10, IL-4, IL-13, IL-5, IL-8, IL-6, and macrophage inflammatory protein (MIP)-3α; plate 2 contained IL-12/IL-23p40, thymus and activation-regulated chemokine (TARC), macrophage-derived chemokine (MDC), monocyte chemotactic protein (MCP)-1, MCP-4, eotaxin, eotaxin-3, MIP-1α, and MIP-1β; and plate 3 contained IL-31, thymic stromal lymphopoietin (TSLP), IL-22, IL-23, and IL-17A/F. Measurements were conducted on a Meso QuickPlex SQ 120 MM (Meso Scale Discovery) according to the manufacturer's instructions. One healthy control sample could not be analyzed. The detection limits are listed in Tables E1 and E2 in the Online Repository (available at www.jacionline.org).

Single-cell RNA sequencing

Single-cell RNA sequencing (scRNA-Seq) data from previous studies from 5 patients with AD, 7 patients with PN, and 3 healthy controls were used.[22] In addition, sequencing data from 3 patients with PSO were acquired via Gene Expression Omnibus (GSE162183).[23] For the AD, PN, and healthy control samples, skin punch biopsy samples were dissolved with a skin dissociation kit from Miltenyi Biotec (San Diego, Calif) for cell isolation.

The isolated cells were immediately processed for scRNA-Seq with a Chromium Single Cell Controller and Single Cell 5' Library & Gel Bead Kits from 10x Genomics (Pleasanton, Calif). CellRanger pipeline v6.1.2 was used for aligning the reads to the GRCH38 human reference genome. The expression matrix was loaded into Seurat v4.3.0 for further downstream analyses. Cells with a high percentage of mitochondrial genes (>12%) and either a very low (<500) or very high number (>6000) of unique genes (nFeature_RNA) were filtered out. Doublets were excluded with doubletFinder v2.0.3. Integration via feature selection and identification of integration anchors was applied. The standard Seurat workflow was applied to process the samples, including principal component analysis (PCA) to identify 20 relevant dimensions through an elbow plot; subsequently, unsupervised clustering was performed with a resolution of 0.5. Cluster visualization was performed with uniform manifold approximation and projection (UMAP).

Statistical analyses

Proteomics. Data from the 2 available technical replicates were averaged for each biological replicate and used as representative values. PCA was performed on summed protein peak areas, and the first 2 principal components were visualized in a scatterplot. Groupwise multivariate *t* distributions were fit to the principal components, and ellipses corresponding to the 95% quantiles were overlaid. Lesional samples were compared with nonlesional samples with paired *t* tests and compared with control samples with Welch *t* test. The resulting *P* values were adjusted for multiple testing with Benjamini-Hochberg correction to control for the false discovery rate. Standardized values of all proteins significantly differentially expressed in any pairwise comparison were displayed (as *z* scores) in a clustered heat map. Clustering of samples and proteins was performed via hierarchical clustering with complete linkage and the Euclidian distance of the standardized expression profiles. Functional enrichment in Gene Ontology (GO; geneontology.org) biological process terms and KEGG (Kyoto Encyclopedia of Genes and Genomes; genome.jp/kegg) pathways were assessed with gene set enrichment tests implemented in clusterProfiler v4.6.2.[24] The gene list was ordered by sign (test statistic) × [$-\log_{10}$(*P* value)]. All gene sets with values between 10 and 500 were tested. The resulting enrichment scores

TABLE I. Patient characteristics

Participant	Age (years)	DLQI	VAS_{10} (itch)	Score	Proteomics	MSD
Atopic dermatitis (AD, n = 6)						
AD1	36	16	8.5	34.9*	Yes	Yes
AD2	79	8	2	13.4	Yes	Yes
AD3	60	15	2	18.5	Yes	Yes
AD4	24	11	6	14.6	Yes	Yes
AD5	21	11	0	16.6	Yes	Yes
AD6	24	8	6	4.8	Yes	Yes
Psoriasis vulgaris (PSO, n = 7)						
PSO1	60	15	8	24.8†	Yes	Yes
PSO2	55	23	8	22.1	Yes	Yes
PSO3	38	29	10	20.9	Yes	Yes
PSO4	54	23	3	5.1	Yes	Yes
PSO5	64	14	5.5	10.1	Yes	Yes
PSO6	73	13	6	4.8	Yes	Yes
PSO7	28	—	6	14.6	Yes	Yes
Prurigo nodularis (PN, n = 6)						
PN1	62	12	6		Yes	Yes
PN2	70	7	7		Yes	Yes
PN3	66	7	8		Yes	Yes
PN4	57	22	8.5		Yes	Yes
PN5	62	18	7		—	Yes
PN6	82	10	7		—	Yes
Controls (C, n = 7)						
C1	42	1	0		Yes	Yes
C2	51	0	0		Yes	Yes
C3	47	1	2		Yes	Yes
C4	25	0	0		Yes	Yes
C5	34	0	1		Yes	Yes
C6	71	0	0		Yes	Yes
C7	37	0	0		Yes	—

DLQI, Dermatology Life Quality Index; *MSD,* Meso Scale Discovery's U-Plex assay; *VAS_{10},* 10-point visual analog scale.
*EASI score was used for AD.
†PASI score was used for PSO.

and *P* values are reported. *P* values were additionally adjusted for multiple testing with Benjamini-Hochberg correction to control for the false discovery rate.[25]

Multiplex electrochemiluminescence cytokine. Calculations, graphs, and comparisons between the lesional samples of each disease group and healthy control skin and between lesional and nonlesional samples within each disease were done on relative effects and tested for significance using the nonpaired or paired version of the permutation-based Brunner-Munzel test[26] in R 4.2.1 (R Project; www.r-project.org). For statistical calculations, values below the determination range were set to zero.

Single-cell RNA sequencing. The significance level was set to alpha = 5% for all statistical tests. All analyses were performed in R v4.2.1 statistical software. Benjamini-Hochberg correction was applied for analyses of scRNA-Seq data.

RESULTS

Proteomics analysis of microdialysate reveals abnormalities in nonlesional skin of patients with AD

MS-based proteome profiling was performed on 6 participants with AD, 7 with PSO, 4 with PN, and 7 healthy controls (Table I). Across all samples, 793 proteins were identified, of which 702 were regularly quantified (see Table E3 in the Online Repository available at www.jacionline.org). Volumes and total protein content of microdialysates did not differ significantly between the groups (see Fig E3 in the Online Repository). After subtraction of proteins attributable to blood microparticles, according to their GO annotations, 517 proteins qualified for further analyses (Fig 1). Among the most differentially expressed gene products were oxysterol binding protein-like 1A (aka OSBPL1A), serpins (SERPINB9, SERPINA1), S100 proteins (S100A7A, S100A8, S100A9), fatty acid binding proteins (FABP4, FABP5), and alpha-1 type I collagen (aka COL1A1) (see Fig E4 in the Online Repository). PCA of the proteomic data indicated overlap of lesional and nonlesional samples from patients with AD and healthy control samples. In PN and PSO, the nonlesional samples overlapped with the control samples, whereas lesional samples showed a greater variation, with distinct principal components with respect to both nonlesional samples and healthy control samples (Fig 2, *A*). We performed further investigation by hierarchical clustering of differentially abundant proteins in lesional skin, nonlesional skin, and healthy control skin for all 3 diseases. For PSO and PN, lesional samples tended to cluster, whereas nonlesional samples overlapped with samples from healthy controls. For AD, no such clustering was observed (Fig 2, *B*). Correlation of proteomic data with clinical parameters such as EASI/PASI or pruritus intensity did not reveal significant associations (data not shown).

We next analyzed differentially abundant proteins from group-wise comparisons for functional enrichment of the top 20 GO biological processes and KEGG pathways. Three of the top 20 enriched GO annotations (nicotinamide adenine dinucleotide

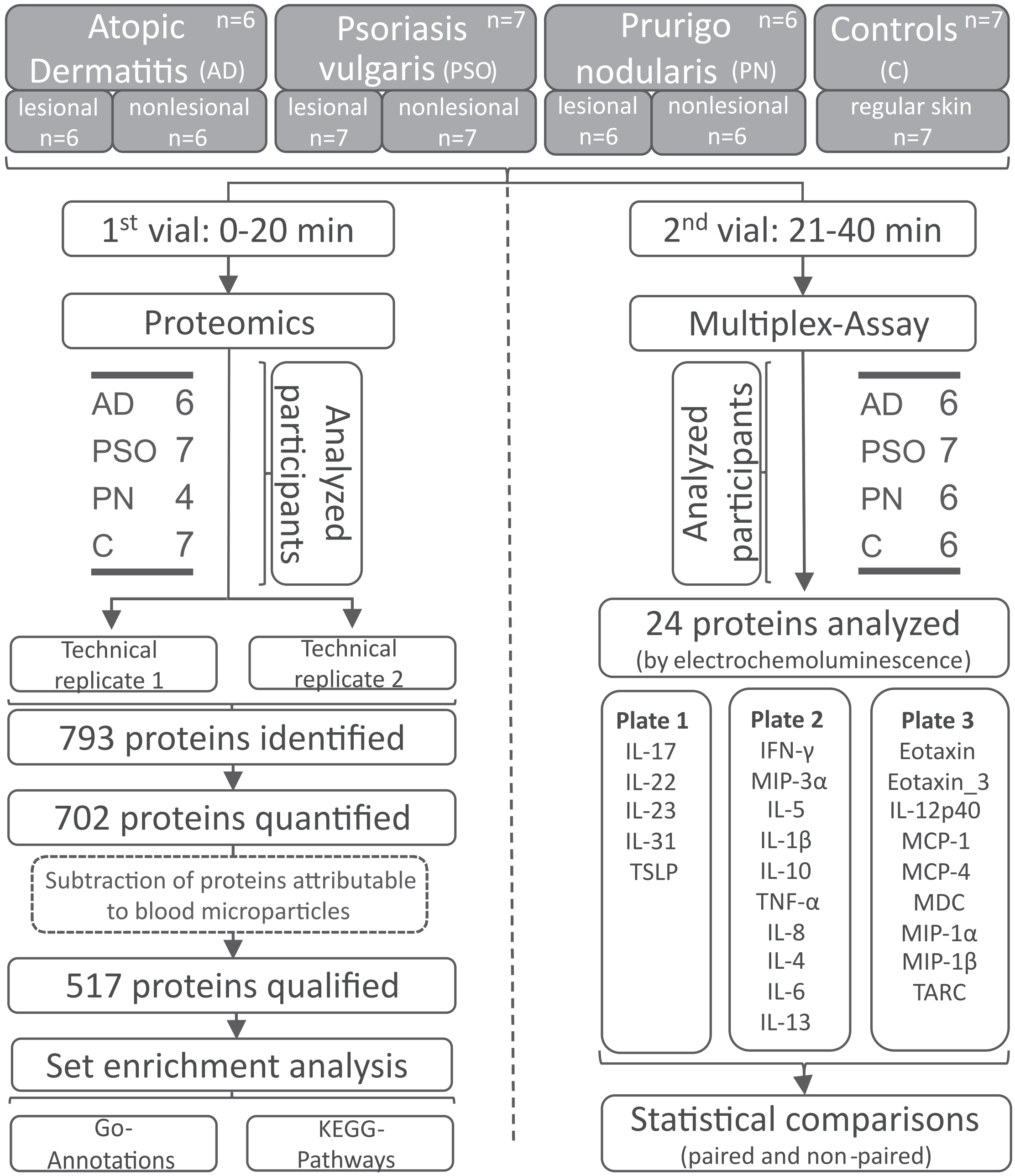

FIG 1. Study outline. Recruited participants with their respective condition are depicted at *top. Below* are processes of proteomic *(left)* and multiplex electrochemiluminescence *(right)* analyses.

[NAD] metabolic process; regulation of secretion by cell; pyruvate metabolic process) overlapped between lesional AD versus control skin, and lesional versus nonlesional AD skin (Fig 3; see Tables E4 and E5 in the Online Repository available at www.jacionline.org). Healthy control samples versus lesional and versus nonlesional AD samples shared only one of the top 20 enriched GO annotations (regulation of hormone levels; see Tables E5 and E6 in the Online Repository). The KEGG pathways enriched between lesional and nonlesional AD skin almost completely overlapped with those in healthy control skin (Fig 3, *A,* and see Tables E13-E15 in the Online Repository). In PSO, 6 of the top 20 GO annotations were significantly overrepresented in lesional skin compared with both nonlesional skin and healthy control skin. The enriched terms included cellular response to stress (Fig 3, and see Tables E7 and E8 in the Online Repository). Correspondingly, 15 of 20 KEGG pathways were enriched in lesional skin compared with either nonlesional skin or healthy control skin (see Tables E16-E18 in the Online Repository). Nonlesional PSO skin was characterized by one overlapping GO annotation also present in lesional skin, but no KEGG pathways overlapped (Fig 3, *B,* and see Tables E7-E9 and E16-E18 in the Online Repository). Similar results were found for PN, for which 5 of the top 20 GO annotations were enriched in lesional skin compared with either nonlesional skin from the same patients or healthy control skin. In nonlesional PN skin versus healthy control skin, no GO annotation was significantly enriched with respect to lesional skin (see Tables E10-E12 in the Online Repository). Likewise, whereas 5 KEGG pathways were enriched in

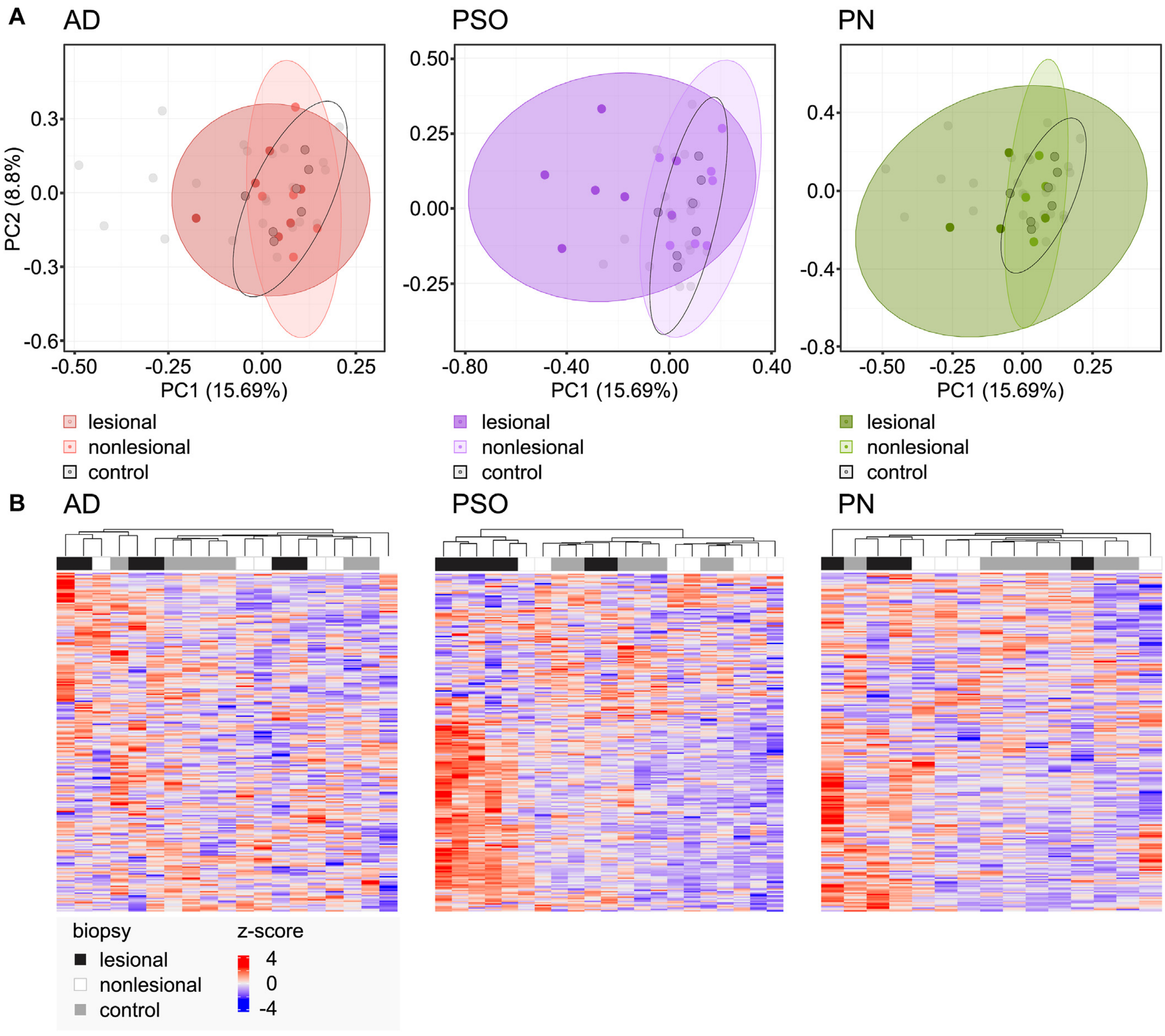

FIG 2. Lesional skin in PSO (n = 7) and PN (n = 4) but not in AD (n = 6) differs from nonlesional skin and skin of healthy controls (n = 7). **(A)** Proteomics data visualized through PCA, with *ellipses* corresponding to 95% quantiles of fitted groupwise multivariate *t* distributions. *Gray* depicts controls, *red* AD, *lilac* PSO, and *green* PN. In each PCA, *darker color* represents lesional skin and *lighter color* nonlesional skin. **(B)** Heat map of hierarchical clustering encompassing all values significantly differing between lesional, nonlesional, and/or control skin for AD *(left)*, PSO *(middle),* and PN *(right)*. In hierarchical clustering, *black* depicts lesional skin, *white* nonlesional skin, and *gray* healthy control skin. *Z* value is visualized on continuous color scale from *blue* (−4) via *white* (0) to *red* (4).

comparisons of lesional PN with either nonlesional PN or healthy control skin, no KEGG pathway was simultaneously enriched in nonlesional PN versus control skin and in lesional PN (Fig 3, *C*, and see Tables E19-E21 in the Online Repository).

Levels of extracellular cytokines IL-12p40, IL-22, IL-8, and MCP-1 may be suitable disease markers

Most customized multiplex cytokine measurements of microdialysis samples were below the lower detection limit (a full list of cytokines and corresponding values within the determination range is provided in Table E2). IL-12p40, IL-22, IL-8, and MCP-1 were widely identified in lesional skin of patients with disease. In healthy controls, almost all cytokine measurements were below the detection limit. In patients with PSO, IL-12p40 was significantly elevated in lesional skin compared with both nonlesional skin and healthy control skin (P = .031 and P = .009, Fig 4, *A*). In AD and PN, IL-12p40 abundance did not differ significantly. IL-22 was significantly elevated in lesional PSO skin compared with both nonlesional or healthy control skin (P = .047 and P = .001, respectively, Fig 4, *B*). Again, no significant results were found for AD or PN. IL-8 was significantly elevated in

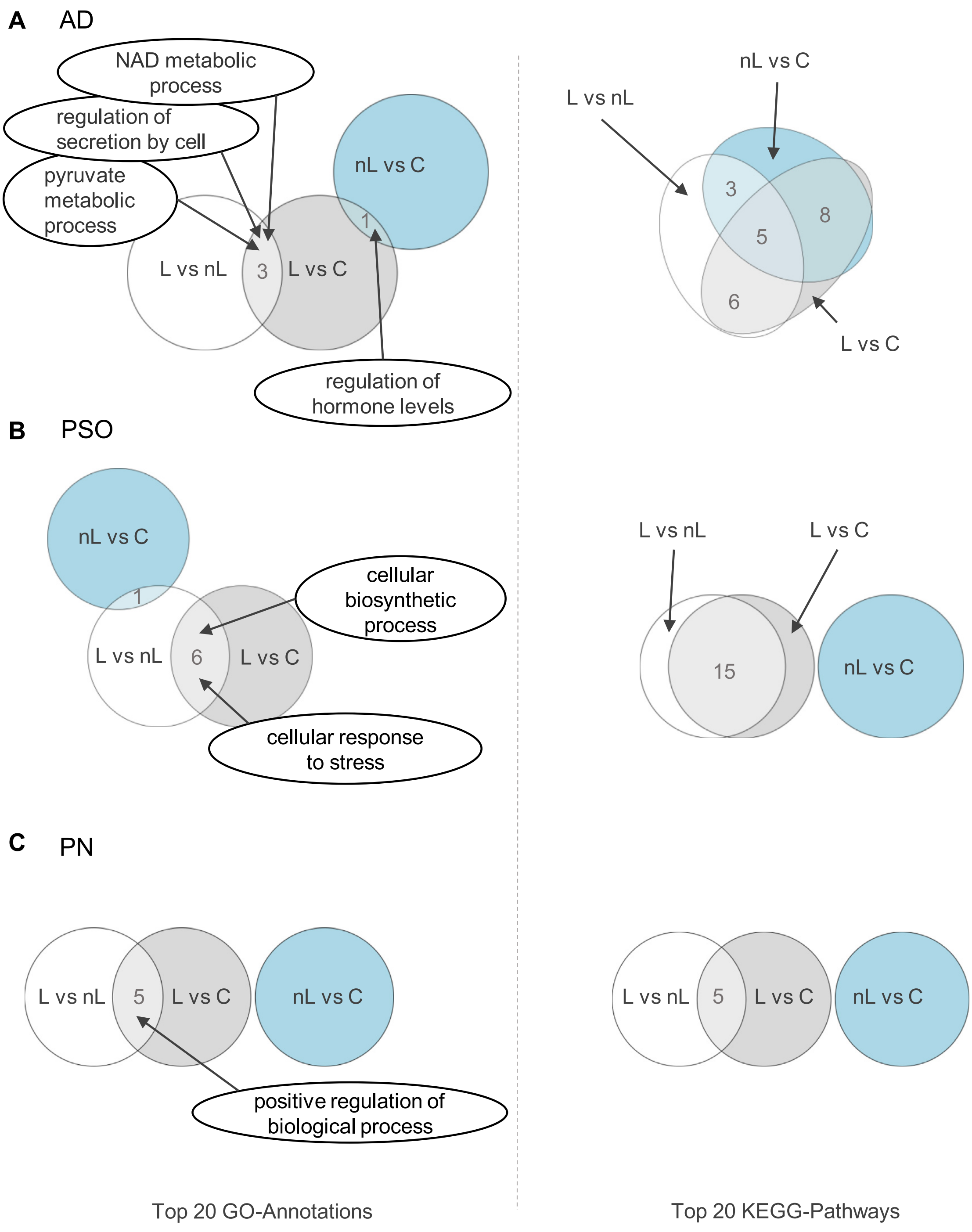

FIG 3. Proteins overexpressed in lesional skin versus nonlesional skin overlap in enriched GO annotations and KEGG pathways with lesional skin versus healthy controls in both PSO and PN. Groupwise comparisons of lesional versus nonlesional, lesional versus control, and nonlesional versus control samples from proteomic data. Significantly over- or underexpressed proteins in these comparisons were analyzed with regard to overlaps in their top 20 enriched GO annotations *(left)* and top 20 enriched KEGG pathways *(right)* and visualized in Euler diagrams.

PSO lesional skin compared with both nonlesional skin and healthy control skin (P = .047 and P = .001, respectively; Fig 4, *C*). In AD, IL-8 was equally significantly elevated in lesional skin compared with both nonlesional and healthy control skin (P = .031 and P = .001, respectively). In PN, lesional skin significantly differed from healthy control skin (P = .002) but not from nonlesional skin. MCP-1 was significantly elevated in skin lesions of patients with PSO compared with both nonlesional skin and healthy control skin (P = .016 and P = .001, Fig 4, *D*). In AD, MCP-1 was significantly elevated in lesional skin only compared with healthy control skin (P = .005) but not to nonlesional skin. Again, no significant differences were found in the samples of

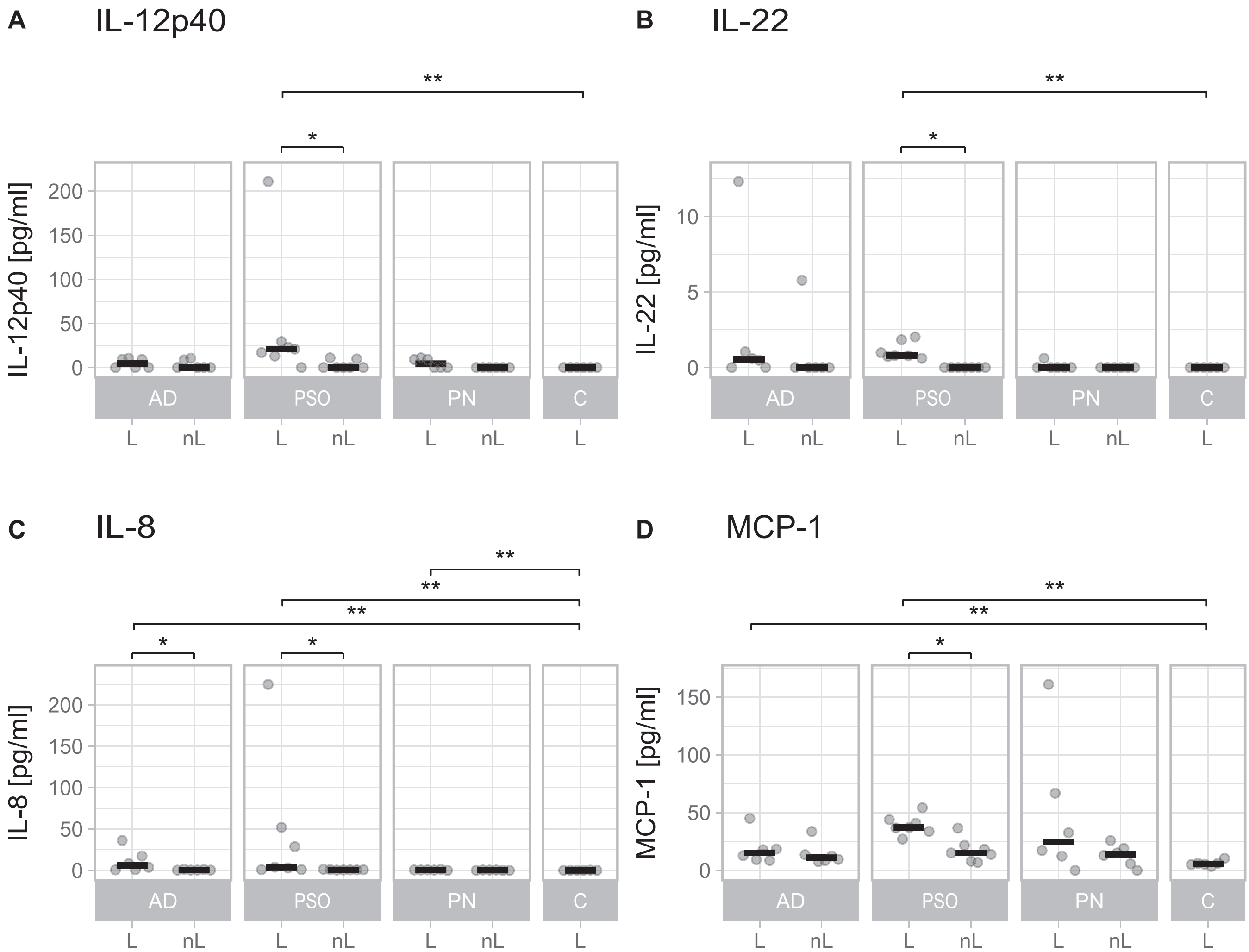

FIG 4. IL-22 and MCP-1 measured by electrochemiluminescence assay are overexpressed in PSO lesional skin versus nonlesional skin (n = 7) and versus healthy controls (n = 6) but not in lesional versus nonlesional AD (n = 6) or PN (n = 6) skin. **(A)** IL-12p40, **(B)** IL-22, **(C)** IL-8, and **(D)** MCP-1 graphs by disease group, subcategorized into lesional (L) and nonlesional (nL) skin. Comparisons between L samples of each disease group and controls and between L and nL samples within each disease were done on relative effects and tested for significance by nonpaired or paired version of permutation-based Brunner-Munzel test; $^{**}P < .01$, $^{*}P < .05$.

patients with PN. TSLP was elevated, although not statistically significantly, in lesions of 3 patients with PSO, but was below the detection limit in corresponding nonlesional samples (see Fig E5 in the Online Repository available at www.jacionline.org). Individual samples contained IL-1β, MCP-4, or macrophage-derived chemokine, but the patient sample size with positive results was too low to yield statistically relevant results (see Figs E6-E8 in the Online Repository).

Identical cellular origin of cytokines in AD, PSO, and PN in integrated scRNA-Seq data from skin biopsy samples

The scRNA-Seq data revealed that *CCL2* (MCP-1) was produced by various cells including endothelial cells, fibroblasts, epithelial cells, and smooth muscle cells (Fig 5). *CXCL8* (IL-8) was produced primarily by antigen-presenting cells in participants with and without disease. We observed no evidence of IL-22 transcripts in scRNA-Seq data of healthy individuals. In AD, PN, and PSO, IL-22 originated from lymphocytes. IL-12B was not detected via scRNA-Seq.

DISCUSSION

The main goal of this study was to assess skin microdialysis as a diagnostic tool for profiling various inflammatory skin diseases. We identified patterns associated with the investigated diseases. Our findings suggest that pathophysiologic changes in PSO and PN are limited to inflammatory lesions, whereas skin alterations in patients with AD also affect nonlesional, noninflamed skin. These data are consistent with previous research findings indicating that hallmarks of AD inflammation occur before, and persist after, clinically visible inflammation has subsided.[11,27-29]

The second focus of this study was to identify unique protein disease profiles locally in skin lesions by comparing skin from patients with AD, PSO, or PN with healthy control skin. Using

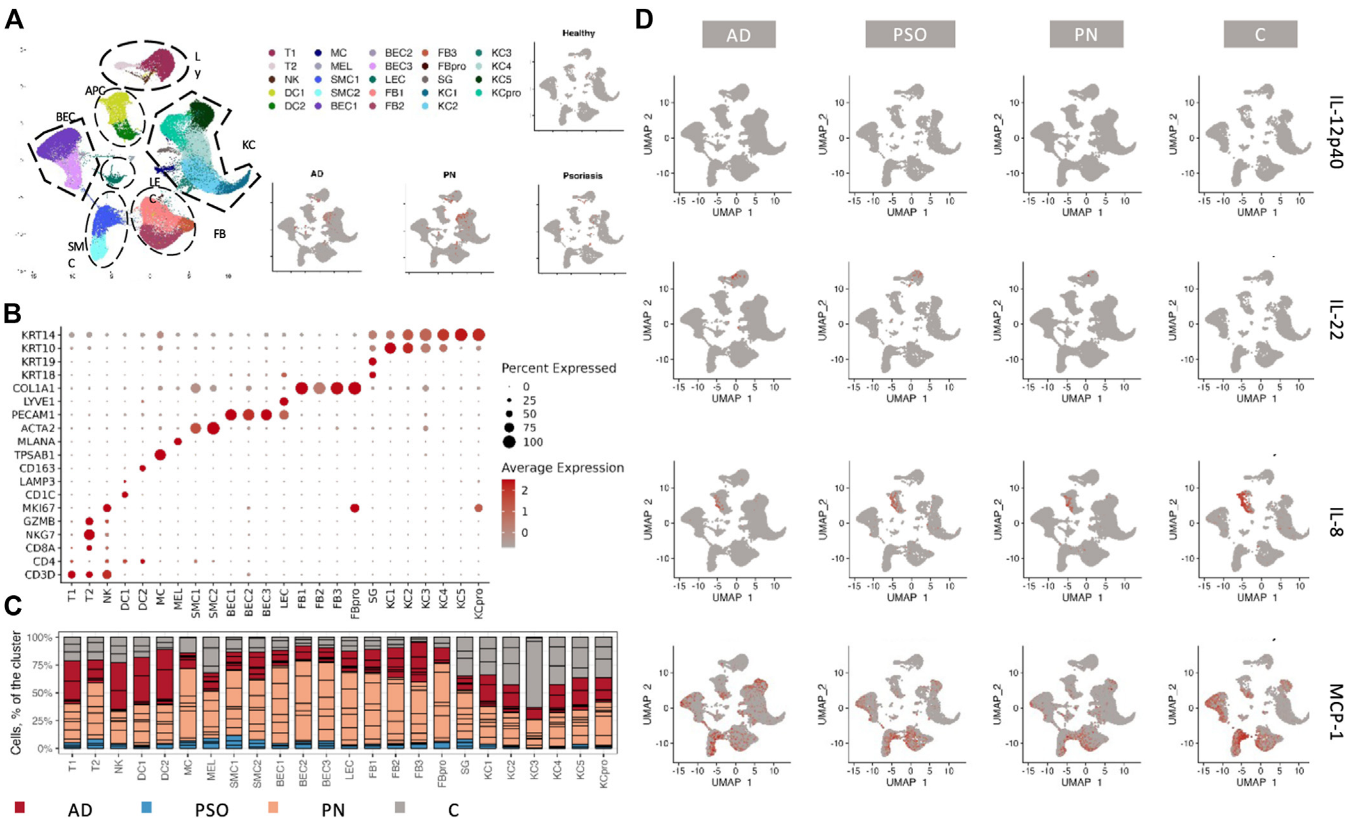

FIG 5. Analysis of scRNA-Seq data revealed that IL-22 originated from lymphocytes and IL-8 from antigen-presenting cells. **(A)** Uniform manifold approximation and projection (UMAP) plot (140,363 cells) of integrated scRNA-Seq data. According to differentially expressed genes, multiple cell clusters were identified: T cells (T1, T2), natural killer (NK) cells, antigen-presenting cells (DC1, DC2), mast cells (MC), melanocytes (MEL), smooth muscle cells (SCM1, SMC2), blood vascular endothelial cells (BEC1, BEC2, BEC3), lymphatic endothelial cells (LEC), fibroblasts (FB1, FB2, FB3, proliferative FB [FBpro]), sebaceous gland (SG) cells, and keratinocytes (KC1, KC2, KC3, KC3, KC5, proliferative KC [KCpro]). Feature plot of proliferating cells marked by MKI67 expression. **(B)** Dot plot of hallmark transcripts expressed by identified clusters. **(C)** Bar chart depicting relative proportion of cells from each disease in every cluster. *Red* indicates AD (n = 5); *blue,* PSO (n = 3); *orange,* PN (n = 7); and *gray,* control (C; n = 3). **(D)** Feature plots showing MCP-1 (CCL2), IL-8 (CXCL8), IL-22, and IL-12p40 (IL-12B)-producing cells in healthy controls, AD, PN, and PSO.

microdialysis, we found that oxysterol binding protein-like 1A (OSBPL1A) expression was more than 10-fold higher in AD compared with PN. Previous research found it decreased in PSO.[30] Contrary to this, alpha-1 type I collagen (COL1A1) was more than 3-fold increased in PN compared with AD or healthy control skin, reflecting fibrotic processes and previous findings from single-cell analyses.[22] We detected 7- to 23-fold increased levels of S100 protein types A7, A8, and A9 in PSO compared with healthy control skin, as expected from other methods.[30] In PN, protease inhibitors of the serpin family were downregulated, while serpin B9 was upregulated more than 5-fold in PSO. In all 3 diseases, fatty acid binding protein (FABP) 5 was upregulated at the expense of FABP4, which was downregulated.

In our study, comparisons of cytokine expression profiles were not possible through proteomic analyses because the resolution of our proteomic approach was insufficient to detect many known cytokines, despite the abovementioned sample processing steps. Of note, other methods of *in situ* transcriptome and proteome analyses also did not register elevated levels of already known central disease mediators in lesional skin—for example, IL-17 or IL-23.[31,32] Furthermore, performing microdialysis on inflamed skin often yielded blood-contaminated dialysates. Visible blood contamination was most prominent in PSO and PN lesions and was mostly absent in nonlesional skin and healthy control skin. Therefore, we subtracted proteins attributable to blood microparticles in our statistical analysis. However, blood contamination due to microlesions seems an inherent problem with this method for analyses of skin with high vascularization, such as PSO skin.

Consequently, we performed protein analyses with the microdialysates by highly sensitive electrochemiluminescence assays. Most assayed cytokines were below the detection limit, possibly because we used the second collection vial obtained during microdialysis. Relevant amounts of cytokines might have been washed out during the first 20 minutes, thus resulting in a lower protein concentration in the second vial collection. Key factors determining the protein concentration in the dialysate are rate of release, binding to high-affinity receptors in tissue,[33] and knowing the diffusion rate in the tissue toward the dialysis membrane, which is lower for larger proteins. Indeed, upregulation of IL-4R on fibroblasts in AD has been demonstrated by single-cell transcriptomics,[34] and therefore upregulation of receptors might have decreased cytokine availability at the microdialysis catheter. We already attempted to account for low protein concentrations by using an assay with high sensitivity (electrochemiluminescence) requiring small sample sizes. This process enabled us to analyze all cytokines without dilution.

The cytokines yielding statistically relevant results included IL-12B, IL-22, C-X-C motif chemokine ligand (CXCL) 8, and MCP-1. Previous research indicated that IL-12B (equivalent to IL-12p40) and IL-1β can be used as biomarkers to guide PSO therapy,[35] and IL-12B can be used to predict disease progression.[36] We found that IL-12p40 was specifically enriched in PSO lesions, and we verified the presence of IL-1β in some of the PSO samples, thus validating our measurements. We further observed MCP-1 (aka chemokine C-C motif ligand [CCL] 2) elevation in PSO lesions compared with nonlesional or healthy control skin, and in AD samples compared with healthy control samples. MCP-1 is a monocyte chemoattractant protein secreted by various cells, including keratinocytes. Its receptor, C-C chemokine receptor 2 (aka CCR2), is expressed on the surfaces of monocytes, and MCP-1 levels are elevated in PSO, AD, and other skin disorders,[37] and in addition show broad upregulation in fibroblasts, keratinocytes, and pericytes[34]—in agreement with our findings. *CXCL8* (IL-8), a chemoattractant for neutrophils, is secreted primarily by antigen-presenting cells. In inflammatory conditions, IL-8 may also be secreted by keratinocytes after stimulation with IL-17A, and its expression is regulated by IL-36, among other cytokines.[38-40] Correspondingly, and in accordance with previous literature,[41] *CXCL8* was elevated in lesional samples of all 3 diseases studied here. Little research has described the role of *CXCL8* in PN. One recent study has indicated *CXCL8* elevation in PN lesions compared with AD lesions through transcriptomic analysis.[42] To our knowledge, our study reports the first data on lesional IL-8 protein levels. In accordance with previous research, we found that IL-8 levels were elevated in lesional skin of both AD and PN. However, we were unable to confirm higher levels in PN lesions than AD lesions, thus extending previous results.[42] Most cytokines were scarce in our PN samples, and statistically significant differences were rarely observed, possibly because of an insufficient number of patients with PN or because extracellular cytokine levels are generally lower in PN than in other diseases such as PSO. Furthermore, IL-22, originating from lymphocytes, was elevated in cytokine measurements of PSO. Greater IL-22 levels in PSO than in healthy control skin were expected, according to the current pathophysiologic understanding of the disease.[43] These considerations demonstrated the integrity of our data. Unfortunately, none of the observed parameters could serve as a novel biomarker to distinguish the 3 diseases or support disease classification. Furthermore, proteomics may not be an ideal tool to detect cytokines, and other tools might be necessary, such as transcriptomics and ELISA. Although extracellular cytokine levels should reflect the type and acuity of inflammatory responses most accurately, paracrine and autocrine signaling combined with an extensive capacity of high-affinity receptors might critically decrease the spillover captured by the microdialysis membrane. Thus, the integrated approach of microdialysis combined with scRNA-Seq appears promising. Further research may combine these techniques within the same patient and additionally focus on the poorly understood role of *CXCL8* in PN.

The main limitation of this study was its small sample size. The sample size did not allow us to differentiate different disease severities or other clinical features of the analyzed lesions. In future studies, including different molecular subtypes of AD, such as type 2–high and type 2–low AD, might be beneficial because these subtypes differ in their cytokine expression profiles.[6] Nummular eczema has been suggested to be a variant of AD with a codominant T_H2/T_H17 immune response; therefore, the researched diseases might have broad and partly overlapping cytokine expression profiles.[44] Such overlap was reflected in our data. In addition, some patients with AD may have high IL-31 levels.[45] Lesional skin of different patients with AD did not cluster well, in contrast to samples from patients with PSO. Not only disease subtypes but also the timing of the microdialysis procedure may influence results. Inflammatory lesions undergo transformation over time. Type 3 immune responses—as seen in PSO, for example—show high plasticity. Over time, type 3–related cells shift toward IFN-γ production, away from type 3 immunity.[2] Disease endotypes and time-dependent plasticity might explain why certain cytokines, such as TSLP, were elevated in lesions in only some of our patients. Keratinocyte-derived TSLP is a prominent protein inducing T_H2 polarization via dendritic cells in the skin.[46] However, TSLP has been found to be elevated in PSO and associated with its pathophysiology.[47-49] This finding may also explain the failure of clinical trials of an antibody to TSLP for treatment of AD.

In conclusion, microdialysis is a promising method through which lesional and nonlesional skin samples can be analyzed, even repetitively. This method yields fluids that can be used for proteomic analyses and protein measurements. However, we did not find evidence that microdialysis can easily differentiate inflammation profiles of different skin diseases. *CXCL8* is elevated in PN, a finding not previously reported. In PN and PSO, inflammation may be limited to lesional skin, whereas in AD, nonlesional skin shows characteristics of lesional skin. Thus, microdialysis may serve as a valuable tool for further understanding the pathophysiology of chronic inflammatory skin diseases.

DISCLOSURE STATEMENT

Supported in part by Kiniksa (San Diego, Calif) and a scholarship from the Deutsche Forschungsgemeinschaft (DFG 413501650 to M.M.H.).

Disclosure of potential conflict of interest: The authors declare that they have no relevant conflicts of interest.

We acknowledge excellent technical support by Meike Schaffrinski. The graphical abstract was created with BioRender.com.

Key messages

- **Microdialysis can be used to analyze inflammatory skin diseases.**
- **Microdialysate can be analyzed using omics or high-sensitivity (multiplex) ELISA.**
- **In PN and PSO, inflammation may be limited to lesional skin, whereas in AD, nonlesional skin shows characteristics of lesional skin.**

REFERENCES

1. Lauffer F, Jargosch M, Krause L, Garzorz-Stark N, Franz R, Roenneberg S, et al. Type I immune response induces keratinocyte necroptosis and is associated with interface dermatitis. J Invest Dermatol 2018;138:1785-94.

2. Annunziato F, Romagnani C, Romagnani S. The 3 major types of innate and adaptive cell-mediated effector immunity. J Allergy Clin Immunol 2015;135:626-35.
3. Ständer S. Atopic dermatitis. N Engl J Med 2021;384:1136-43.
4. Treudler R, Simon J. Developments and perspectives in allergology. J Dtsch Dermatol Ges 2023;21:399-403.
5. Gieseck RL, Wilson MS, Wynn TA. Type 2 immunity in tissue repair and fibrosis. Nat Rev Immunol 2018;18:62-76.
6. Akdis CA, Arkwright PD, Brüggen MC, Busse W, Gadina M, Guttman-Yassky E, et al. Type 2 immunity in the skin and lungs. Allergy 2020;75:1582-605.
7. Schön MP, Berking C, Biedermann T, Buhl T, Erpenbeck L, Eyerich K, et al. COVID-19 and immunological regulations—from basic and translational aspects to clinical implications. J Dtsch Dermatol Ges 2020;18:795-807.
8. Czarnowicki T, He H, Krueger JG, Guttman-Yassky E. Atopic dermatitis endotypes and implications for targeted therapeutics. J Allergy Clin Immunol 2019;143:1-11.
9. Schäbitz A, Eyerich K, Garzorz-Stark N. So close, and yet so far away: the dichotomy of the specific immune response and inflammation in psoriasis and atopic dermatitis. J Intern Med 2021;290:27-39.
10. Lauffer F, Eyerich K. Eczematized psoriasis—a frequent but often neglected variant of plaque psoriasis. J Dtsch Dermatol Ges 2023;21:445-53.
11. Brunner PM, Emerson RO, Tipton C, Garcet S, Khattri S, Coats I, et al. Nonlesional atopic dermatitis skin shares similar T-cell clones with lesional tissues. Allergy 2017;72:2017-25.
12. Langan SM, Irvine AD, Weidinger S. Atopic dermatitis. Lancet 2020;396(10247): 345-60.
13. Steinhoff M, Ahmad F, Pandey A, Datsi A, AlHammadi A, Al-Khawaga S, et al. Neuroimmune communication regulating pruritus in atopic dermatitis. J Allergy Clin Immunol 2022;149:1875-98.
14. Agelopoulos K, Renkhold L, Wiegmann H, Dugas M, Süer A, Zeidler C, et al. Transcriptomic, epigenomic, and neuroanatomic signatures differ in chronic prurigo, atopic dermatitis, and brachioradial pruritus. J Invest Dermatol 2023;143:264-72.e3.
15. Garzorz-Stark N, Krause L, Lauffer F, Atenhan A, Thomas J, Stark SP, et al. A novel molecular disease classifier for psoriasis and eczema. Exp Dermatol 2016;25:767-74.
16. Schmelz M, Luz O, Averbeck B, Bickel A. Plasma extravasation and neuropeptide release in human skin as measured by intradermal microdialysis. Neurosci Lett 1997;230:117-20.
17. Baumann KY, Church MK, Clough GF, Quist SR, Schmelz M, Skov PS, et al. Skin microdialysis: methods, applications and future opportunities—an EAACI position paper. Clin Transl Allergy 2019;9:24.
18. Papoiu ADP, Wang H, Nattkemper L, Tey HL, Ishiuji Y, Chan YH, et al. A study of serum concentrations and dermal levels of NGF in atopic dermatitis and healthy subjects. Neuropeptides 2011;45:417-22.
19. Hughes CS, Moggridge S, Müller T, Sorensen PH, Morin GB, Krijgsveld J. Single-pot, solid-phase–enhanced sample preparation for proteomics experiments. Nat Protoc 2019;14:68-85.
20. Zhang Y, Bilbao A, Bruderer T, Luban J, Strambio-De-Castillia C, Lisacek F, et al. The use of variable Q1 isolation windows improves selectivity in LC-SWATH-MS acquisition. J Proteome Res 2015;14:4359-71.
21. Lambert JP, Ivosev G, Couzens AL, Larsen B, Taipale M, Lin ZY, et al. Mapping differential interactomes by affinity purification coupled with data-independent mass spectrometry acquisition. Nat Methods 2013;10:1239-45.
22. Alkon N, Assen FP, Arnoldner T, Bauer WM, Medjimorec MA, Shaw LE, et al. Single-cell RNA sequencing defines disease-specific differences between chronic nodular prurigo and atopic dermatitis. J Allergy Clin Immunol 2023;152:420-35.
23. Gao Y, Yao X, Zhai Y, Li L, Li H, Sun X, et al. Single cell transcriptional zonation of human psoriasis skin identifies an alternative immunoregulatory axis conducted by skin resident cells. Cell Death Dis 2021;12:450.
24. Yu G, Wang LG, Han Y, He QY. clusterProfiler: an R package for comparing biological themes among gene clusters. Omics J Integr Biol 2012;16:284-7.
25. Subramanian A, Tamayo P, Mootha VK, Mukherjee S, Ebert BL, Gillette MA, et al. Gene set enrichment analysis: a knowledge-based approach for interpreting genome-wide expression profiles. Proc Natl Acad Sci 2005;102:15545-50.
26. Pauly M, Asendorf T, Konietschke F. Permutation-based inference for the AUC: a unified approach for continuous and discontinuous data. Biom J 2016;58:1319-37.
27. Sirvent S, Vallejo AF, Corden E, Teo Y, Davies J, Clayton K, et al. Impaired expression of metallothioneins contributes to allergen-induced inflammation in patients with atopic dermatitis. Nat Commun 2023;14:2880.
28. Pavel AB, Renert-Yuval Y, Wu J, Del Duca E, Diaz A, Lefferdink R, et al. Tape strips from early-onset pediatric atopic dermatitis highlight disease abnormalities in nonlesional skin. Allergy 2021;76:314-25.
29. Suárez-Fariñas M, Tintle SJ, Shemer A, Chiricozzi A, Nograles K, Cardinale I, et al. Nonlesional atopic dermatitis skin is characterized by broad terminal differentiation defects and variable immune abnormalities. J Allergy Clin Immunol 2011;127:954-64.e4.
30. Rioux G, Simard M, Morin S, Lorthois I, Guérin SL, Pouliot R. Development of a 3D psoriatic skin model optimized for infiltration of IL-17A producing T cells: focus on the crosstalk between T cells and psoriatic keratinocytes. Acta Biomater 2021;136:210-22.
31. Frost B, Schmidt M, Klein B, Loeffler-Wirth H, Krohn K, Reidenbach T, et al. Single-cell transcriptomics reveals prominent expression of IL-14, IL-18, and IL-32 in psoriasis. Eur J Immunol 2023;53:2250354.
32. Schäbitz A, Hillig C, Mubarak M, Jargosch M, Farnoud A, Scala E, et al. Spatial transcriptomics landscape of lesions from non-communicable inflammatory skin diseases. Nat Commun 2022;13:7729.
33. Thurley K, Gerecht D, Friedmann E, Höfer T. Three-dimensional gradients of cytokine signaling between T cells. PLoS Comput Biol 2015;11:e1004206.
34. He H, Suryawanshi H, Morozov P, Gay-Mimbrera J, Del Duca E, Kim HJ, et al. Single-cell transcriptome analysis of human skin identifies novel fibroblast subpopulation and enrichment of immune subsets in atopic dermatitis. J Allergy Clin Immunol 2020;145:1615-28.
35. Corbett M, Ramessur R, Marshall D, Acencio ML, Ostaszewski M, Barbosa IA, et al. Biomarkers of systemic treatment response in people with psoriasis: a scoping review. Br J Dermatol 2022;187:494-506.
36. Ramessur R, Corbett M, Marshall D, Acencio ML, Barbosa IA, Dand N, et al. Biomarkers of disease progression in people with psoriasis: a scoping review. Br J Dermatol 2022;187:481-93.
37. Behfar S, Hassanshahi G, Nazari A, Khorramdelazad H. A brief look at the role of monocyte chemoattractant protein-1 (CCL2) in the pathophysiology of psoriasis. Cytokine 2018;110:226-31.
38. Furue M, Kadono T. "Inflammatory skin march" in atopic dermatitis and psoriasis. Inflamm Res 2017;66:833-42.
39. Nedoszytko B, Sokołowska-Wojdyło M, Ruckemann-Dziurdzińska K, Roszkiewicz J, Nowicki R. Chemokines and cytokines network in the pathogenesis of the inflammatory skin diseases: atopic dermatitis, psoriasis and skin mastocytosis. Adv Dermatol Allergol Dermatol Alergol 2014;31:84-91.
40. Ogawa E, Sato Y, Minagawa A, Okuyama R. Pathogenesis of psoriasis and development of treatment. J Dermatol 2018;45:264-72.
41. Zhou Z, Meng L, Cai Y, Yan W, Bai Y, Chen J. Exploration of the potential mechanism of the common differentially expressed genes in psoriasis and atopic dermatitis. Biomed Res Int 2022;2022:1177299.
42. Deng J, Parthasarathy V, Marani M, Bordeaux Z, Lee K, Trinh C, et al. Extracellular matrix and dermal nerve growth factor dysregulation in prurigo nodularis compared to atopic dermatitis. Front Med 21;9:1022889.
43. Boehncke WH, Schön MP. Psoriasis. Lancet 2015;386(9997):983-94.
44. Böhner A, Jargosch M, Müller NS, Garzorz-Stark N, Pilz C, Lauffer F, et al. The neglected twin: nummular eczema is a variant of atopic dermatitis with co-dominant Th2/Th17 immune response. J Allergy Clin Immunol 2023;152: 408-19.
45. Cevikbas F, Wang X, Akiyama T, Kempkes C, Savinko T, Antal A, et al. A sensory neuron-expressed IL-31 receptor mediates T helper cell–dependent itch: involvement of TRPV1 and TRPA1. J Allergy Clin Immunol 2014;133:448-60.
46. Traidl S, Roesner L, Zeitvogel J, Werfel T. Eczema herpeticum in atopic dermatitis. Allergy 2021;76:3017-27.
47. Li SZ, Jin XX, Shan Y, Jin HZ, Zuo YG. Expression of thymic stromal lymphopoietin in immune-related dermatoses. Mediators Inflamm 2022;2022: 9242383.
48. Suwarsa O, Dharmadji HP, Sutedja E, Herlina L, Sori PR, Hindritiani R, et al. Skin tissue expression and serum level of thymic stromal lymphopoietin in patients with psoriasis vulgaris. Dermatol Rep 2019;11:8006.
49. Volpe E, Pattarini L, Martinez-Cingolani C, Meller S, Donnadieu MH, Bogiatzi SI, et al. Thymic stromal lymphopoietin links keratinocytes and dendritic cell–derived IL-23 in patients with psoriasis. J Allergy Clin Immunol 2014;134: 373-81.e4.